Journal of The Electrochemical Society, **148** (11) A1260-A1265 (2001)
0013-4651/2001/148(11)/A1260/6/$7.00 © The Electrochemical Society, Inc.

Electrochemical Properties of Carbonaceous Thin Films Prepared by Plasma Chemical Vapor Deposition

Tomokazu Fukutsuka, Takeshi Abe,* Minoru Inaba,* and Zempachi Ogumi*,z

Graduate School of Engineering, Kyoto University, Sakyo-ku Kyoto 606-8501, Japan

Carbonaceous thin films were prepared from acetylene and argon by plasma-assisted chemical vapor deposition (plasma CVD). The carbonaceous thin films were characterized mainly by scanning electron microscope (SEM) and Raman spectroscopy. Then their electrochemical properties were studied by cyclic voltammetry, charge-discharge measurements, and linear sweep voltammetry. From the SEM image carbonaceous thin films appeared flat and pinhole free. Crystallinity of carbonaceous thin films are affected by the applied rf power from Raman spectra. The difference of the applied rf power also affected the results of cyclic voltammetry and charge-discharge measurements. The lithium ion storage mechanism of carbonaceous thin film is discussed from the results of electrochemical measurements.
 [DOI: 10.1149/1.1409542]

Manuscript submitted August 7, 2000; revised manuscript received June 4, 2001. Available electronically October 8, 2001.

Lithium-ion batteries have been extensively studied because of their high performance and potentialities. Carbonaceous materials with sp^2-type structure have attracted much attention for use as negative electrodes of lithium ion batteries. Among them, highly crystallized graphite has been employed as the negative electrode for lithium-ion batteries in the commercial market. However, various carbonaceous materials have been extensively investigated so far as negative electrode materials for improving the performance of lithium-ion batteries.[1-9]

Since carbonaceous materials are generally powders, binders are essential for the preparation of electrodes, which makes it difficult to elucidate the precise electrochemical properties of the carbonaceous materials themselves. For the study of carbonaceous negative electrodes, thin films are very useful, because the films can be used as electrodes without binders and furthermore, it is easy for us to evaluate their electrode surface area. However, few studies employing carbonaceous thin films as negative electrodes of lithium-ion batteries have been made.[10] This is because there are some difficulties in preparing thin-film electrodes of the sp^2-type carbonaceous materials due to low adherence on a substrate, etc.

A plasma is an ionized gas containing equal numbers of positive and negative charges, and a number of nonionized neutral excited species. Glow discharge plasma is unique in that it can generate chemically very reactive species at low temperatures due to the nonequilibrium nature of the plasma state. Plasma-assisted chemical vapor deposition (CVD) has been used for the preparation of a variety of inorganic materials.[11,12] The chemical reactions are accelerated in plasma at low temperatures, and plasma CVD can easily give dense and pinhole free films.

Synthesis of carbonaceous thin films by use of plasma CVD has been also carried out by many workers. However, most of these studies have focused on the preparation of diamond films and/or diamond-like carbon films of sp^3-type structure,[13,14] and little attention has been paid to a synthesis of sp^2-type carbonaceous thin films.

Preparation and characterization of sp^2-type carbonaceous thin films by plasma CVD have been already reported by the present authors.[15-17] In this work, electrochemical properties of carbonaceous thin-film electrodes prepared by plasma CVD were studied by cyclic voltammetry (CV), charge-discharge measurements, and linear sweep voltammetry.

Experimental

Figure 1 shows a schematic diagram of the plasma CVD apparatus used in this study. Starting materials were acetylene and argon. Acetylene and argon were selected as the carbon source and the plasma assist gas, respectively. Substrates were placed on a ground electrode whose temperature was kept at 873 K. Carbonaceous thin films were deposited on substrates of nickel and Pyrex® glass sheets. Glow discharge plasma was generated between rf and ground electrodes by an rf power supply of 13.56 MHz, and the applied rf power was changed from 10 to 90 W. Flow rates of argon and acetylene were set at 20 and 10 sccm, respectively. The total pressure of the reaction chamber was kept at 133 Pa.

The resultant carbonaceous films were characterized by scanning electron microscopy (SEM, Hitachi S-510) and Raman spectroscopy. The Raman spectra were excited by using a 514.5 nm line (50 mW) of an argon ion laser (NEC, GLG3260), and the scattered light was collected in a backscattering geometry. All spectra were recorded using a spectrometer (Jobin-Yvon, T64000) equipped with a multichannel charge coupled device (CCD) detector. Each measurement was carried out at room temperature with an integration time of 300 s.

Electrochemical measurements were performed by using a three-electrode electrochemical cell. Lithium metal was used as counter and reference electrodes, and the electrolyte solution was a mixture (1:1 by volume) of ethylene carbonate (EC) and diethyl carbonate

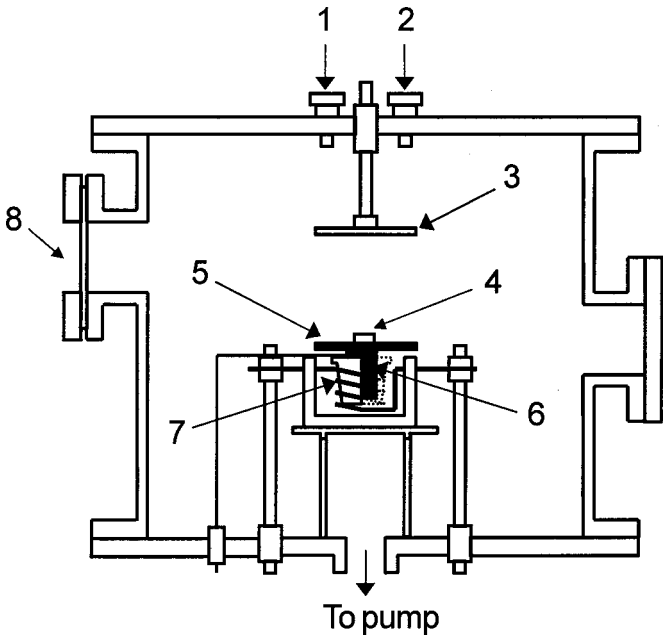

Figure 1. Schematic of rf reactor for the plasma CVD apparatus. 1, Ar inlet: 2, C_2H_2 inlet; 3, rf electrode; 4, substrate; 5, thermocouple; 6, ground electrode; 7, tungsten heater; 8, viewport.

* Electrochemical Society Active Member.
z E-mail: ogumi@scl.kyoto-u.ac.jp

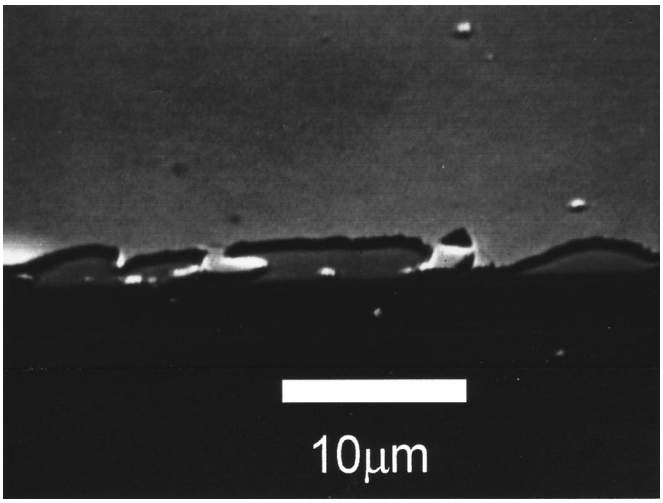

Figure 2. SEM image of carbonaceous thin film prepared by plasma CVD. Reaction time, 6 h; substrate, Pyrex® glass, applied rf power, 10 W.

(DEC) containing 1 mol dm^{-3} $LiClO_4$ (battery grade by Mitsubishi Petrochemical Company, Limited). The cell was assembled in an argon-filled glove box. Electrochemical properties were examined by cyclic voltammetry and linear sweep voltammetry (Radiometer, VoltaLab 32) and charge-discharge measurements using a battery test system (Hokuto Denko, HJ101SM6). Unless otherwise stated, the potential is described *vs.* Li/Li^+.

Results and Discussion

Surface morphology of carbonaceous thin films.—Figure 2 shows a typical SEM image of carbonaceous thin film prepared by plasma CVD at 10 W. From the image, the surface of the carbonaceous thin film was very flat and free from pinholes. The film thickness was determined to be less than 1 μm by cross section of SEM image. Carbonaceous thin films prepared using other rf powers also gave morphologies similar to those using an rf power of 10 W.

Raman spectroscopy of carbonaceous thin films.—Raman spectra of carbonaceous thin films are shown in Fig. 3. Three main peaks around 1360, 1580, and 1620 cm^{-1} were observed. The peak around 1580 cm^{-1} is well known to be related to the crystallinity of carbonaceous materials, and is assigned to the Raman active E_{2g} mode frequency (G band).[18] The peak around 1360 cm^{-1} is ascribed to the Raman inactive A_{1g} mode frequency.[18] Peaks around 1360 and 1620 cm^{-1} appear in the case of finite crystal size and imperfections of carbonaceous materials,[19] and the former is called a D band and the latter is a D′ band. As is given in Fig. 3, the peak around 1580 cm^{-1} of the G band became sharper, and its position shifted toward 1580 cm^{-1} with increasing the applied rf power. Full width at half maximum (fwhm) of the peak around 1580 cm^{-1} was reported to be correlated with the crystallinity of carbonaceous materials,[19] and single crystals of graphite gave only one peak around 1580 cm^{-1}. Hence, the result in Fig. 3 indicates that crystallinity of the samples increased with increasing the applied rf power, which was also confirmed by the conductivity measurements.[15] The important point of the spectra was that crystallinity of carbonaceous thin film can be easily changed by the applied rf power at a fixed temperature as low as 873 K. In other words, high rf power plasma results in the high electron temperature, leading to large energy transfer to carbonaceous thin film at a fixed temperature. In Raman spectra, peak intensities around 1360 cm^{-1} are higher than those around 1580 cm^{-1}. This feature indicates that the films contained nongraphitized carbon to some extent.[20] From this result, carbonaceous thin films in this study were composed of the graphitized structures with partly nongraphitized structures.

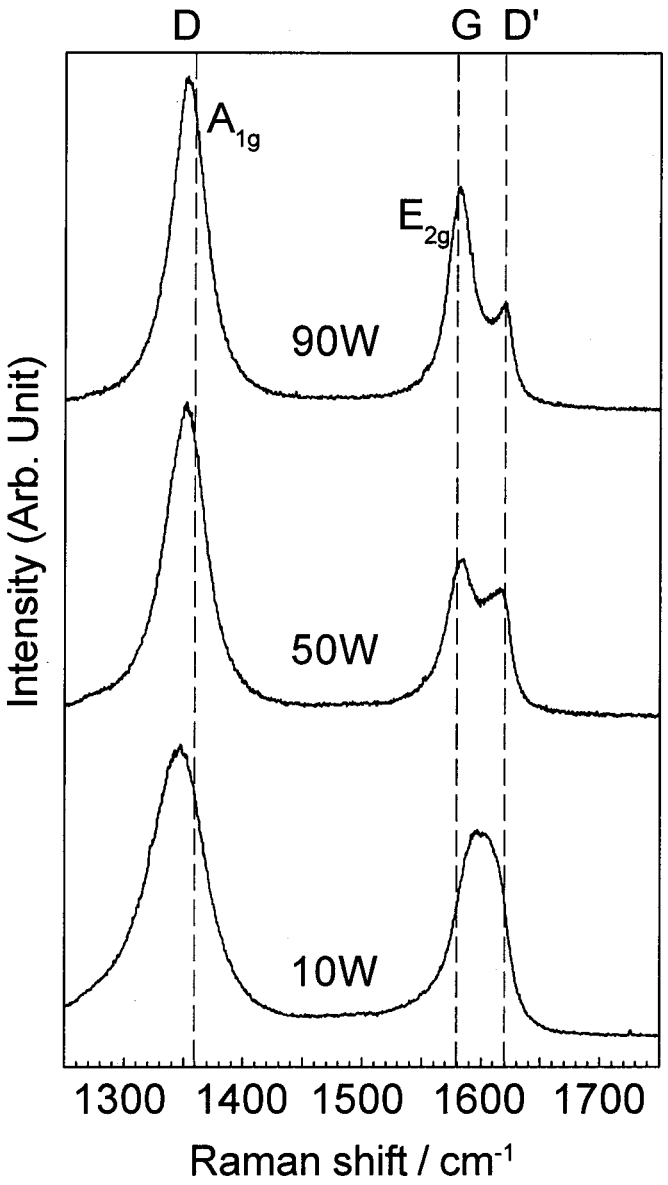

Figure 3. Raman spectra of carbonaceous thin films prepared by plasma CVD. Reaction time, 6 h; substrate, Ni; applied rf power, 10, 50, and 90 W.

Cyclic voltammogram of carbonaceous thin films.—Figure 4 shows cyclic voltammograms of carbonaceous thin film prepared at 90 W. The cyclic voltammogram was measured with a sweep rate of 1 mV/s in the potential range of 0 to 3 V. For the first sweep, a large irreversible reduction was observed from the potential around 1.5 to 0.5 V. However, it almost disappeared after the second sweep as is evident from Fig. 4. These results indicate that the decomposition of the solvent and formation of the solid electrolyte interface (SEI) on the surface of carbonaceous thin films should occur effectively.[21,22] For all the carbonaceous films prepared at any rf powers, large reduction currents at around 1.5-0.5 V appeared at the first cycle of cyclic voltammograms.

Figure 5 shows cyclic voltammograms at the second sweep for carbonaceous thin films prepared by rf powers of 10 and 90 W. Electrochemical properties were found to be different between carbonaceous thin films prepared at 10 and 90 W as shown in Fig. 5. In the oxidation process, the peak of carbonaceous thin film prepared at 90 W was sharp and had a clear shoulder around 0.1-0.2 V as shown by the arrow in the insertion, while the peak was broad and did not have such a clear shoulder for the film prepared at 10 W. In the

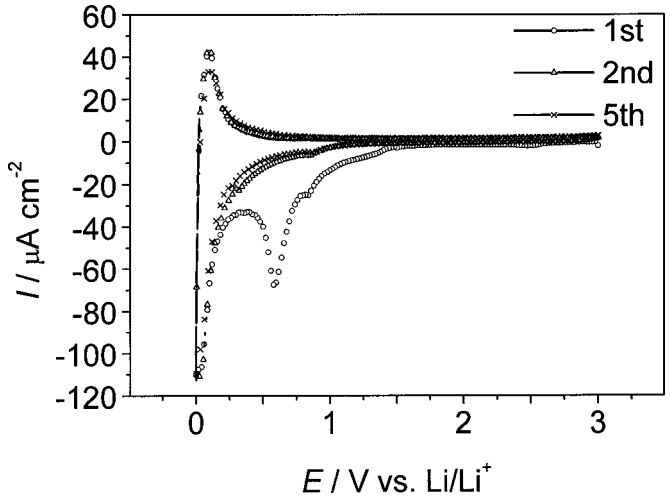

Figure 4. Cyclic voltammograms of carbonaceous thin film in 1 mol dm^{-3} $LiClO_4$/EC + DEC (1:1). Sweep rate, 1 mV/s; reaction time, 6 h; substrate, Ni; applied rf power, 90 W.

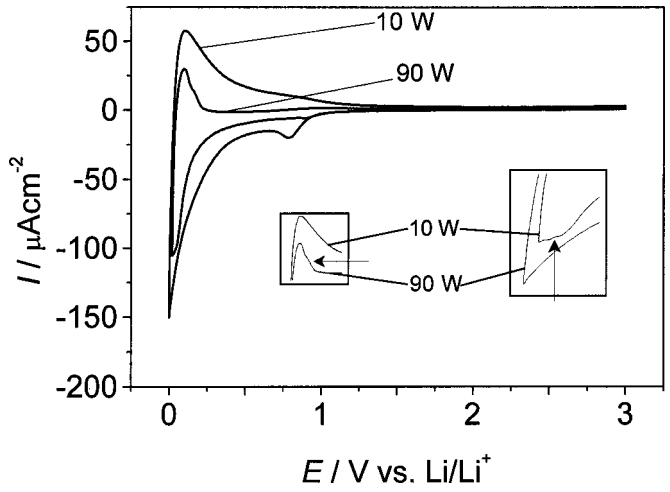

Figure 5. Cyclic voltammograms (2nd cycle) of carbonaceous thin films in 1 mol dm^{-3} $LiClO_4$/EC + DEC (1:1). Sweep rate, 1 mV/s, applied rf power, 10 and 90 W.

reduction process, the peak at 90 W had a clear shoulder around 0.1 V as shown by an arrow in the insertion, but the peak near 0 V for the film prepared at 10 W was very smooth. These results were correlated with the formation of stage structures of Li-GICs.[23] The difference in the shape of cyclic voltammograms were also related with Raman spectra shown in Fig. 3, that is, crystallinity of the film prepared at 90 W was higher than that of the film prepared at 10 W. In other words, the degree of crystallinity of the carbonaceous thin films affected the shapes of cyclic voltammograms. From the above results, the intercalation and deintercalation behavior of carbonaceous thin films was found to be dependent on the applied rf powers.

Charge and discharge characteristics of carbonaceous thin films.—Figure 6a shows charge and discharge characteristics of carbonaceous thin film prepared at 10 W. At the first cycle (inset figure), a very large irreversible capacity above 0.5 V appeared. The large irreversible capacity is also reported for other carbonaceous materials.[24] This irreversible capacity decreased dramatically after the second cycle. The insertion curve of the sample prepared at 10 W showed about 1100 mAh/g of capacity at the second cycle and the extraction curve showed about 600 mAh/g. In the extraction

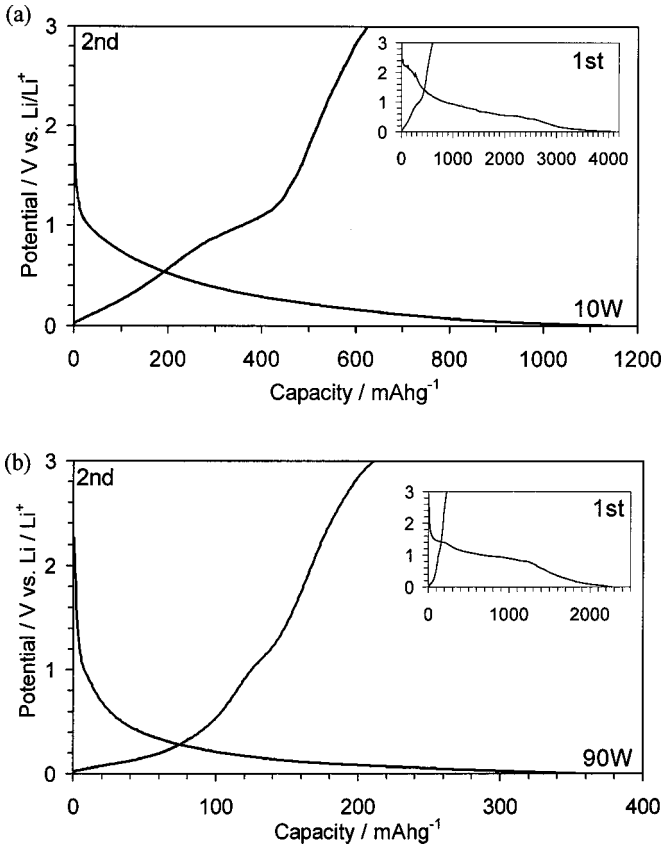

Figure 6. Charge and discharge characteristics (2nd cycle) of carbonaceous thin films in 1 mol dm^{-3} $LiClO_4$/EC + DEC (1:1). Applied rf power (a) 10 and (b) 90 W. The inset figure is charge and discharge characteristics of 1st cycle.

curves, a comparatively large potential plateau appeared at approximately 1 V. These results indicated that the electrochemical properties of carbonaceous thin film prepared at 10 W was very similar to those for graphitizable carbon heat-treated at lower temperatures.[25] Figure 6b shows charge and discharge characteristics of a carbonaceous thin film prepared at 90 W. At the first cycle (inset figure), a very large irreversible capacity above 0.5 V also appeared as is observed for the film prepared at 10 W. The insertion curve of the sample prepared at 90 W showed about 350 mAh/g of capacity at the second cycle, and the extraction curve showed about 200 mAh/g. On the extraction curves, a very small potential plateau appeared at approximately 1 V. A small plateau appeared below the potential of 0.25 V. In the case of graphite, deintercalation of lithium ion from Li-GIC takes place below 0.25 V,[26] and therefore this result should be correlated with the formation of stage structures of Li-GIC. From these results, charge and discharge characteristics showed tendencies similar to the results of cyclic voltammograms for carbonaceous thin films in this study. The ratio of the capacity in the potential range 0 to 0.25 V to that in the range 0.25 to 3 V was evaluated to be 0.185 for the sample at 10 W and 0.498 for sample at 90 W. Tatsumi *et al.* reported that this ratio of capacity became large with increasing crystallinity of the mesocarbon microbeads (MCMBs).[27] Hence, the present results of charge-discharge measurements support the idea that the high rf power gave a film of high crystallinity.

Mechanism of insertion and extraction of lithium ion for carbonaceous thin films.—As is mentioned above, the electrochemical behaviors for the insertion and extraction of lithium ions for the present carbonaceous thin films are different from those for graphite, but are similar to those for graphitizable carbon heat-treated at lower temperatures.[25] To examine the details of insertion and extraction of

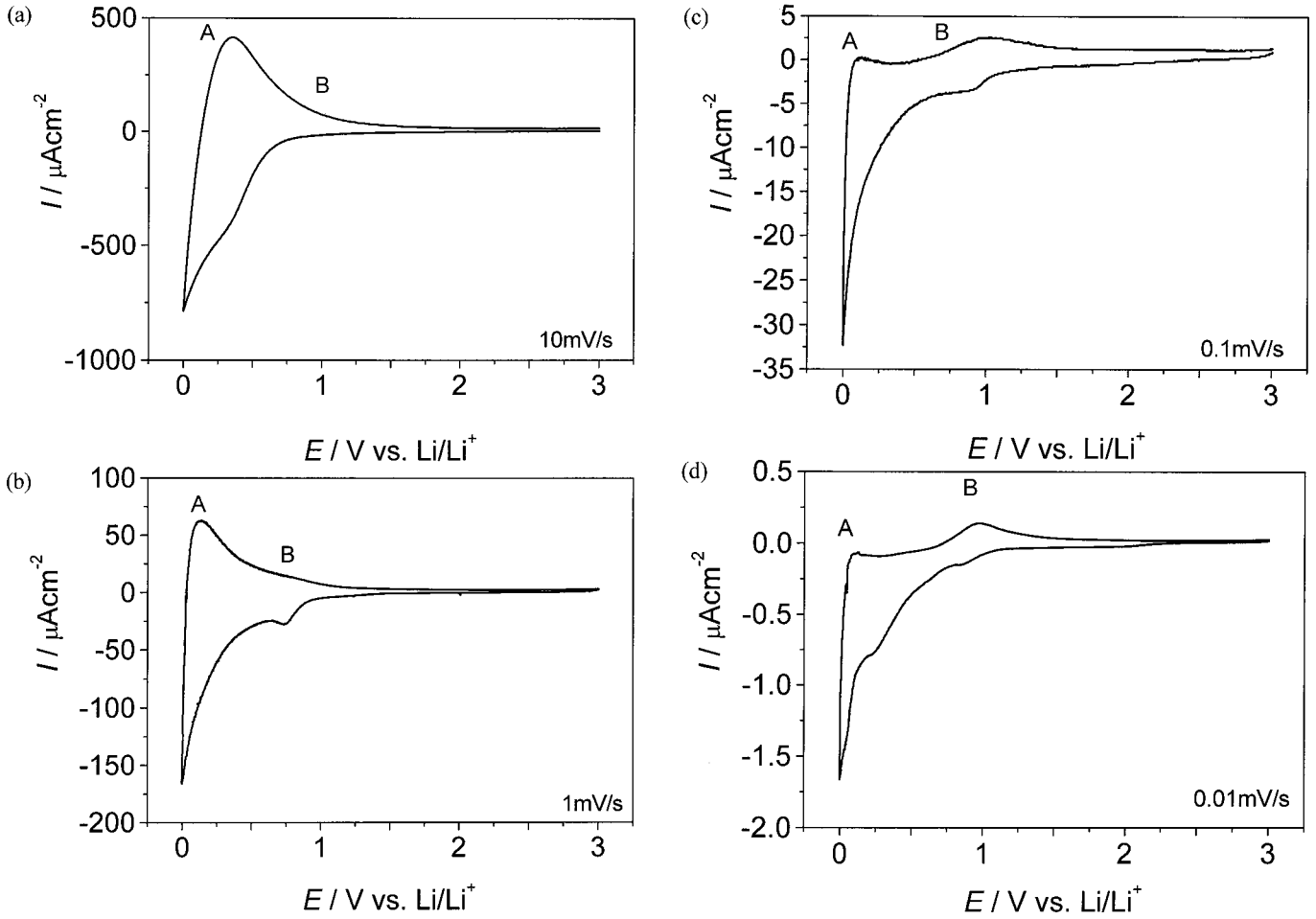

Figure 7. Cyclic voltammograms (2nd cycle) of carbonaceous thin films prepared by plasma CVD. Applied rf power, 10 W; sweep rate, (a) 10, (b) 1, (c) 0.1, and (d) 0.01 mV/s.

lithium ion of the carbonaceous thin films, cyclic voltammetry was conducted at various sweep rates. Figures 7a-d show cyclic voltammograms at the second sweep of the sample prepared at 10 W. Sweep rates are (a) 10, (b) 1, (c) 0.1, and (d) 0.01 mV/s. As given in Fig. 7, a change of sweep rate influences not only values of magnitudes of current but also shapes of cyclic voltammograms; the peak of the oxidation current around 0.1-0.2 V is relatively large and that around 0.9-1.0 V is very small at higher sweep rates, while the peak around 0.1-0.2 V is small and the peak around 0.9-1.0 V is large at lower sweep rates. By considering the previous literature,[25] oxidation peaks around 0.1-0.2 V, denoted as A in Fig. 7, are due to deintercalation of the lithium ion stored in graphene layers and that peaks around 0.9-1.0 V, denoted as B, are ascribed to the extraction of lithium ion stored in some sites except for graphene layers. In Fig. 7, the ratio of peak B to peak A increases with decreasing the sweep rates. A similar tendency was obtained for the sample prepared at 90 W. These results mean that extraction of a potential around 0.9-1.0 V is kinetically influenced. This is also obvious by charge-discharge measurements obtained at different current densities as shown in Fig. 8. Figure 8 shows charge and discharge characteristics at the second cycle of carbonaceous thin films prepared at 10 W by two current densities (a) 263 and (b) 26.0 mA/g. In Fig. 8, the capacity of (a) is very different from that of (b). This is because the current density for (a) is so large that utilization efficiency of carbonaceous thin film becomes small, leading to a smaller capacity of (a) than that of (b). There is no plateau at around 1 V for the extraction curve in Fig. 8a, while a clear plateau can be seen in Fig. 8b, indicating that no capacity around 1 V is available for the large current densities, which is in good agreement with results as given in Fig. 7a-d.

Next, the lithium ion entities, which can be extracted at around 1 V, are focused by linear sweep voltammetry.

The lithium ion was inserted by sweeping the electrode potentials from 3.0 to 0.3, 0.1, and 0 V, followed by keeping the above potentials for 10 h, and then the potential was reversibly swept linearly to 3.0 V. Figure 9 shows positive linear sweep voltammograms of carbonaceous thin films prepared at 10 W with a sweep rate of 0.1 mV/s. As shown in Fig. 9, the electrodes kept at 0.1 V (dashed line) and 0.3 V (dotted line) did not give any peak at around 1 V, while the electrode kept at 0 V (solid line) exhibited a clear peak around 1 V.

The above results indicated that lithium ion inserted into the carbonaceous thin films at 0 V can be extracted both at about 0 and 1 V. If the lithium ion insertion and extraction was a simple redox reaction, the reduction peak at about 1 V should appear even at the higher sweep rate (Fig. 7a), but that was not the case. Thus the present lithium ion insertion and extraction are not a simple reaction, which led us to consider another lithium ion insertion and extraction mechanism.

The above discussion leads to the fact that transfer of lithium ion from site A to site B is necessary for the lithium ion to insert into site B. Otherwise the lithium ion must directly insert into site B. However, linear sweep voltammetry clearly shows that no insertion of lithium ion at around 1 V occurred. Figures 7 and 8 clearly show

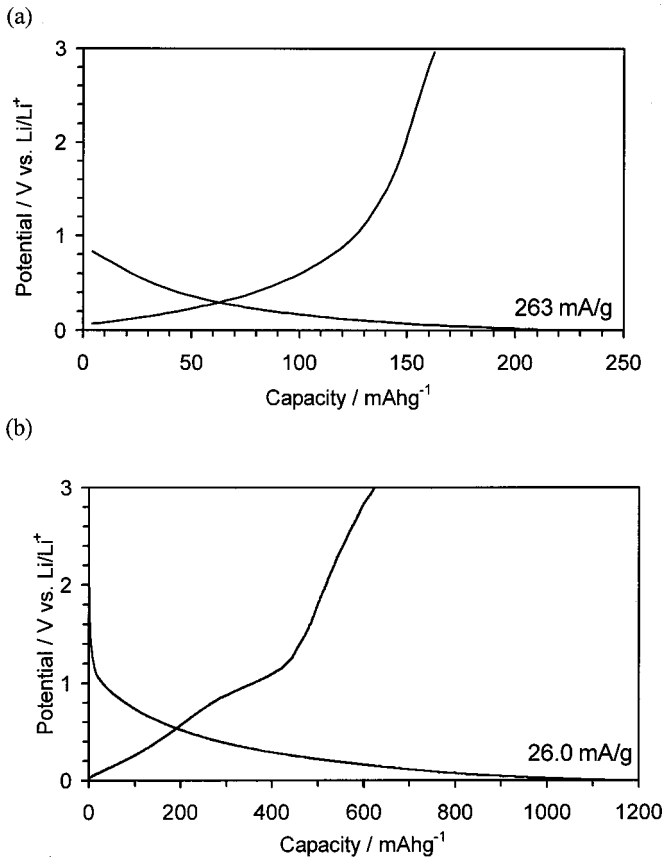

Figure 8. Charge and discharge characteristics of carbonaceous thin films at the 2nd charge-discharge cycle in 1 mol dm^{-3} $LiClO_4$/EC + DEC (1:1). Applied rf power, 10 W; current density, (a) 263 and (b) 26.0 mA/g.

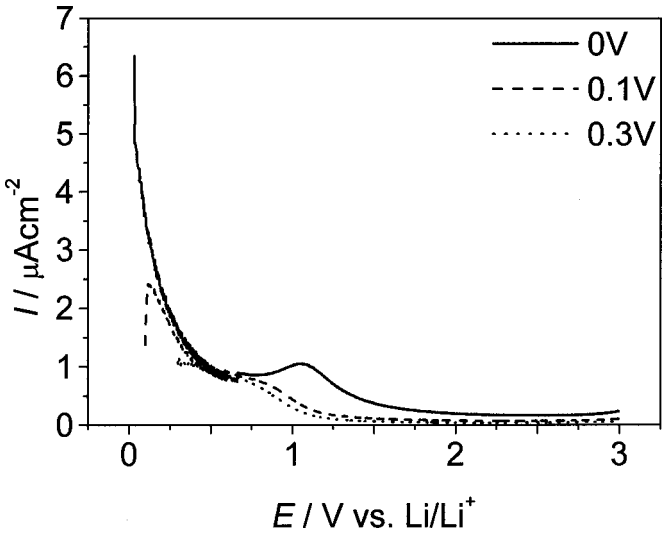

Figure 9. Linear sweep voltammograms (2nd sweep) of carbonaceous thin films prepared by plasma CVD in 1 mol dm^{-3} $LiClO_4$/EC + DEC (1:1). Applied rf power: 10 W. Sweep rate 0.1 mV/s.

that the extraction of lithium ion from site B only occurs at the lower sweep rate and the smaller current density, indicating that the activation energy should be large for the lithium ion transfer from site A to site B and that the transfer is a slow reaction. In other words, site B occupied by the lithium ion is thermodynamically more stable than site A, which is in excellent agreement with the literature.[28,29]

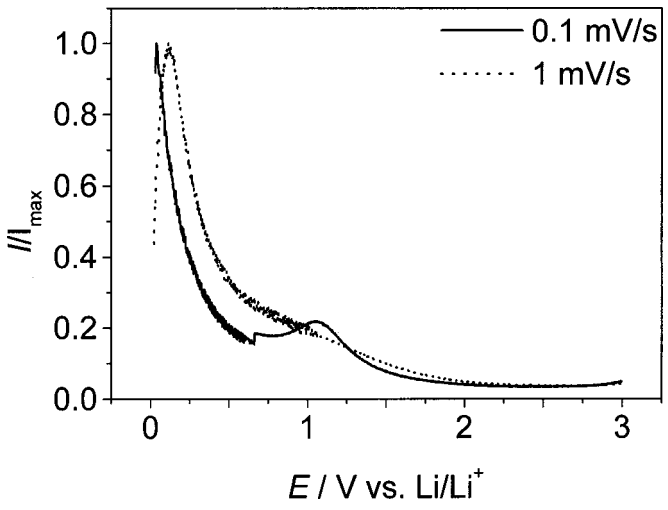

Figure 10. Linear sweep voltammograms of carbonaceous thin film prepared by plasma CVD in 1 mol dm^{-3} $LiClO_4$/EC + DEC (1:1). Applied rf power, 10 W; sweep rate, 0.1 mV/s for 2nd cycle, and 1 mV/s for 3rd cycle. Each voltammograms is normalized by maximum peak height.

To further clarify that extraction of lithium ion from site B is a slow process, linear sweep voltammetry with different sweep rates was conducted. Prior to linear sweep voltammetry, the carbonaceous thin film was scanned from 3 to 0 V, and held at these potential of 0 V for 10 h. Figure 10 shows linear sweep voltammograms of a carbonaceous thin film electrode prepared at 10 W at two sweep rates of 0.1 mV/s (second cycle, solid line) and 1 mV/s (third cycle, dotted line). Each voltammogram is normalized by the maximum peak height. A broad peak appeared near 1 V at the sweep rate of 0.1 mV/s, while no peak appeared at the rate of 1 mV/s. This result indicates that no extraction of lithium ion from site B occurs at a high sweep rate, leading to the conclusion again that extraction of lithium ion from site B is a slow process.

The above results suggest that there should be an activation process of lithium ion transfer from site A to site B. The insertion and extraction mechanisms in this work can be summarized by Fig. 11. Here, vertical axis represents the total energy against reaction coordinates. At first, lithium ion intercalates into site A as shown by Fig. 11(2). After site A is mostly filled by lithium ion, the electrode potential should reach about 0 V and the transfer of lithium ion from site A to site B occurs, probably accompanied by heat generation

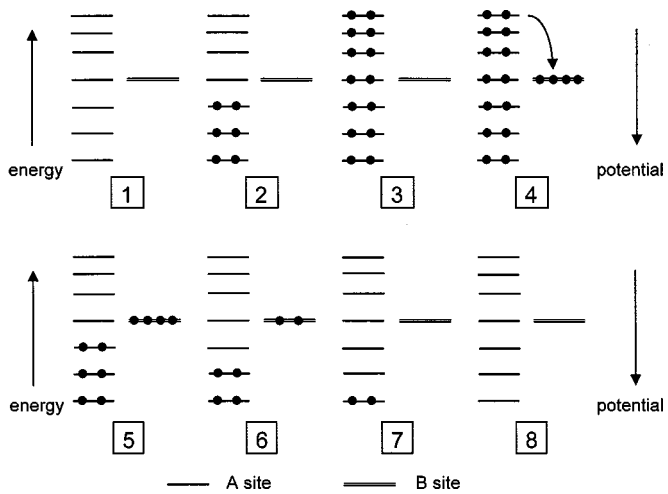

Figure 11. An energy state model to explain lithium ion insertion and extraction of carbonaceous thin films.

due to the energy gap between site A and site B [Fig. 11(3) and (4)].[30] During lithium ion transfer from site A to site B, insertion of the lithium ion into site A through the electrolyte occurs simultaneously. Finally, site A and site B, are filled with lithium ions. As is shown in Fig. 11(5), site A filled with lithium ion is thermodynamically more unstable than site B filled with lithium ion, and hence deintercalation of lithium ion proceeds from site A. When the deintercalation of lithium ion from site A occurs, the electrode potential for site A becomes more positive, and then, site A becomes thermodynamically more stable than site B filled with lithium ion. Then lithium ion is extracted from the B sites [Fig. 11(6)]. There are two possible routes for extraction of lithium ion from site B. One route is that lithium ions extract directly from site B with a slow process. Another route is that lithium ions transfer again from site B to site A accompanied by heat generation again and are extracted through site A. It has recently been shown by Inaba *et al.*[30] the reasons for hysteresis in the charge-discharge profiles of mesocarbon microbeads heat-treated at lower temperatures by calorimetric study.[30] They observed heat generation during lithium extraction.[30] Hence, the latter route is more probable.

The above mechanism for lithium ion insertion and extraction is in good agreement with that reported by Zheng *et al.*[31] In the case of large current densities, lithium insertion and extraction proceeds by $1 \rightarrow 2 \rightarrow 3 \rightarrow 7 \rightarrow 8$. For small current densities and keeping 0 V for enough time, the reaction of lithium and carbonaceous thin films occurs by $1 \rightarrow 2 \rightarrow 3 \rightarrow 4 \rightarrow 5 \rightarrow 6 \rightarrow 7 \rightarrow 8$.

Conclusions

Carbonaceous thin films were prepared by C_2H_2/Ar glow discharge plasma. Carbonaceous thin films in this study were homogeneous and pinhole free. RF power of the plasma was found to influence the crystallinity of carbonaceous thin films. The lithium ion storage in different sites for the resultant carbonaceous thin films was clarified by using cyclic voltammetry, charge-discharge measurements, and linear sweep voltammetry. Carbonaceous materials give various electrochemical properties for use in lithium-ion batteries, and our present carbonaceous thin films can be regarded as a model of carbonaceous materials heat-treated at lower temperatures.

Acknowledgments

This work was financially supported by a Grant-in-Aid for Scientific Research (no. 11555238) from the Ministry of Education, Science, Sports and Culture, Japan, and CREST of JST (Japan Science and Technology).

Kyoto University assisted in meeting the publication costs of this article.

References

1. J. R. Dahn, T. Zheng, Y. Liu, and J. S. Xue, *Science*, **270**, 590 (1995).
2. J. R. Dahn, A. K. Sleigh, H. Shi, J. N. Reimers, Q. Zhong, and B. M. Way, *Electrochim. Acta*, **38**, 1179 (1993).
3. N. Imanishi, H. Kashiwagi, T. Ichikawa, Y. Takeda, O. Yamamoto, and M. Inagaki, *J. Electrochem. Soc.*, **140**, 315 (1993).
4. I. Mochida, C.-H. Ku, S.-H. Yoon, and Y. Korai, *J. Power Sources*, **75**, 214 (1998).
5. T. Zheng, J. S. Xue, and J. R. Dahn, *Chem. Mater.*, **8**, 389 (1996).
6. M. Inaba, Z. Shiroma, A. Funabiki, and Z. Ogumi, *Langmuir*, **12**, 1535 (1996).
7. M. Inaba, H. Yoshida, Z. Ogumi, T. Abe, Y. Mizutani, and M. Asano, *J. Electrochem. Soc.*, **142**, 20 (1995).
8. M. Inaba, H. Yoshida, and Z. Ogumi, *J. Electrochem. Soc.*, **143**, 2572 (1996).
9. Y.-S. Han, J.-S. Yu, G.-S. Park, and J.-Y. Lee, *J. Electrochem. Soc.*, **146**, 3999 (1999).
10. M. Mohri, N. Yanagisawa, Y. Tajima, T. Tanaka, T. Mitate, S. Nakajima, M. Yoshida, M. Yoshimoto, T. Suzuki, and H. Wada, *J. Power Sources*, **26**, 545 (1989).
11. N. Awaya and Y. Arita, *Jpn. J. Appl. Phys., Part 1*, **30**, 1813 (1991).
12. E. Kny, L. L. Levenson, W. J. James, and R. A. Auerbach, *Thin Solid Films*, **85**, 23 (1981).
13. S. Matsumoto, *J. Mater. Sci. Lett.*, **4**, 600 (1985).
14. J. C. Angus and C. C. Hayman, *Science*, **241**, 913 (1988).
15. T. Abe, T. Fukutsuka, M. Inaba, and Z. Ogumi, *Carbon*, **37**, 1165 (1999).
16. T. Fukutsuka, T. Abe, M. Inaba, and Z. Ogumi, *Tanso*, **190**, 252 (1999).
17. T. Fukutsuka, T. Abe, M. Inaba, and Z. Ogumi, *Mol. Cryst. Liq. Cryst. Sect. A*, **340**, 517 (2000).
18. F. Tuinstra and J. L. Koenig, *J. Chem. Phys.*, **53**, 1126 (1970).
19. G. Katagiri, *Tanso*, **175**, 304 (1996).
20. D. S. Knight and W. B. White, *J. Mater. Res.*, **4**, 385 (1989).
21. E. Peled, *J. Electrochem. Soc.*, **126**, 2047 (1979).
22. J. O. Besenhard, M. Winter, J. Yang, and W. Biberacher, *J. Power Sources*, **51**, 228 (1995).
23. R. Takagi, T. Okubo, K. Sekine, and T. Takamura, *Denki Kagaku oyobi Kogyo Butsuri Kagaku*, **65**, 333 (1997).
24. I. Mochida, C.-H. Ku, M. Egashira, and M. Kimura, *Denki Kagaku oyobi Kogyo Butsuri Kagaku*, **66**, 1281 (1998).
25. A. Mabuchi, K. Tokumitsu, H. Fujimoto, and T. Kasuh, *J. Electrochem. Soc.*, **142**, 1041 (1995).
26. T. Ohzuku, Y. Iwakoshi, and K. Sawai, *J. Electrochem. Soc.*, **140**, 2490 (1993).
27. K. Tatsumi, N. Iwashita, H. Sakaebe, H. Shioyama, S. Higuchi, A. Mabuchi, and H. Fujimoto, *J. Electrochem. Soc.*, **142**, 716 (1995).
28. S.-J. Lee, T. Itoh, M. Nishizawa, K. Yamada, and I. Uchida, *Denki Kagaku oyobi Kogyo Butsuri Kagaku*, **66**, 1276 (1998).
29. S.-J. Lee, M. Nishizawa, and I. Uchida, *Electrochim. Acta*, **44**, 2379 (1999).
30. M. Inaba, M. Fujikawa, T. Abe, and Z. Ogumi, *J. Electrochem. Soc.*, **147**, 4008 (2000).
31. T. Zheng, W. R. McKinnon, and J. R. Dahn, *J. Electrochem. Soc.*, **143**, 2137 (1996).